PROCEEDINGS OF SCIENCE

Luminosity Measurements with the ATLAS Inner Detector in Run 3 of the LHC

Filippo Dattola[a,*] **on behalf of the ATLAS collaboration**

[a] *Deutsches Elektronen-Synchrotron (DESY), Notkestrasse 85, 22607 Hamburg, Germany*

E-mail: filippo.dattola@desy.de

Luminosity is a fundamental parameter in any particle collider, linking measured event rates to cross sections of physics processes. In this contribution, the key ingredients of the ATLAS luminosity determination are outlined, with a focus on measurements performed with the Inner Detector in Run 3 of the LHC. The performance of the well-established track-counting algorithm is discussed, together with the results of the track-counting-based luminosity correction procedure applied in standard data-taking conditions. Alongside track counting, the initial development of a novel algorithm, measuring luminosity by counting clusters in the Pixel Detector, is presented. The optimisation of the cluster selection for luminosity measurements is discussed, together with preliminary studies of the algorithm performance and background characterisation.

The European Physical Society Conference on High Energy Physics (EPS-HEP2025)
7-11 July 2025
Marseille, France

*Speaker

 ISSN 1824-8039 . Published by SISSA Medialab.

PoS(EPS-HEP2025)278

1. Luminosity measurement with the ATLAS detector

A precise measurement of the integrated luminosity is an essential requirement of the ATLAS physics programme at the CERN Large Hadron Collider (LHC) [1, 2]. At the LHC, the luminosity corresponding to the crossing of a single pair of proton bunches can be expressed as

$$\mathcal{L}_b = \frac{\mu \cdot f_r}{\sigma_{\text{inel}}}, \tag{1}$$

where μ is the pileup parameter, representing the average number of inelastic interactions per bunch crossing (BC), f_r is the LHC revolution frequency, and σ_{inel} is the proton-proton (pp) inelastic cross section. Summing $\mathcal{L}_b$ over the BCs occuring in the LHC ring, each denoted by a specific *bunch crossing identifier* (BCID), the resulting luminosity can be written in terms of the pileup parameter averaged over all colliding bunch pairs, $\langle\mu\rangle$, as

$$\mathcal{L} = \sum_{\text{BCIDs}} \frac{\mu(\text{BCID}) \cdot f_r}{\sigma_{\text{inel}}} = \frac{\langle\mu\rangle \cdot f_r \cdot n_{\text{B}}}{\sigma_{\text{inel}}}, \tag{2}$$

with n_{B} being the number of filled proton bunches. However, the algorithms based on the luminosity-sensitive detectors in ATLAS (*luminometers*) can only measure a visible interaction rate, $\mu_{\text{vis}} = \epsilon\mu$, corresponding to a fraction of the total inelastic interactions, such that

$$\mathcal{L} = \frac{\langle\mu\rangle_{\text{vis}} \cdot f_r \cdot n_{\text{B}}}{\sigma_{\text{vis}}}, \tag{3}$$

where $\sigma_{\text{vis}} = \epsilon\sigma_{\text{inel}}$ corresponds to the visible cross section, usually determined in dedicated beam-separation scans, called van-der-Meer (vdM) scans [5]. The integrated luminosity is obtained by integration of $\mathcal{L}$ over time. The smallest time interval used for ATLAS luminosity measurements is a Time Block (TB) of ~ 60 s in which $\mathcal{L}$ and the data-taking conditions are assumed to be stable. The reference luminometer in Run 3 is the LUCID-2 Cherenkov detector (hereafter LUCID) [6]. It is used in combination with other independent luminometers, which have complementary capabilities and different systematic uncertainties. The individual measurements are combined in an analysis consisting of three main components.

- The σ_{vis} calibration of LUCID performed via vdM scans in low-luminosity fills ($\mu \sim 0.5$), under specially tailored LHC conditions, characterised by isolated bunches and no crossing angle.

- Transfer of the vdM calibration to the physics data-taking regime at high luminosity and correction of nonlinearities.

- Analysis of the calibration stability over time, performed via relative comparisons of the luminosities measured by different luminometers.

For the pp collision data collected at a centre-of-mass energy of $\sqrt{s} = 13$ TeV in Run 2, ATLAS achieved a record uncertainty of 0.83% [3], and the goal for Run 3 is a final uncertainty within 1%.

2. Luminosity with Track Counting

Track Counting (TC) is the ATLAS luminosity algorithm determining μ_{vis} from offline measurements of the mean number of reconstructed tracks per bunch crossing. Randomly triggered colliding bunch crossings are sampled, and only data from the ATLAS silicon tracking detectors (SCT and Pixel [8]) are read out, typically at 200 Hz in normal physics data-taking conditions and up to $\sim$ 50 kHz during vdM scans and other special runs. Tracks used in TC measurements are reconstructed offline with dedicated settings and are required to satisfy specific selection criteria optimised for luminosity monitoring [3]. The linearity of track counting with changing μ conditions is used to validate and correct the LUCID response at high μ. The validation of the vdM calibration transfer to the high-luminosity physics regime is performed by comparing LUCID and TC, after normalising TC to LUCID in the same LHC fills as the vdM scans, utilising periods with stable, almost constant luminosity where the beams are colliding head-on in ATLAS. As shown in Figure 1a, in physics regime LUCID overestimates luminosity by up to $\sim$ 10%, mostly due to signal migration effects [3]. The TC measurement, which has been observed to be more robust than LUCID against variations in μ [3], is then used to derive a correction of the form

$$\langle \mu_{\text{corr}} \rangle = p_0 \langle \mu_{\text{uncorr}} \rangle + p_1 (\langle \mu_{\text{uncorr}} \rangle)^2 \, . \tag{4}$$

Here $\langle \mu_{\text{uncorr}} \rangle$ is the uncorrected and $\langle \mu_{\text{corr}} \rangle$ is the corrected LUCID $\langle \mu \rangle$ value, and the parameters p_0 and p_1 are obtained from the linear fit to the TC-to-LUCID ratio shown Figure 1a. This TC-based luminosity correction is derived from up to 10 physics runs taken in the vicinity of the vdM-scan period and is then applied to LUCID measurements in all other runs of the same data-taking year. After the correction, the run-integrated luminosity measured by LUCID is typically in agreement with TC, and with calorimeter-based luminosity measurements, within ±0.5%, as shown in Figure 1b. Here, localised larger variations between LUCID and other luminometers are due to non-standard LHC conditions.

The stability of the TC measurement is monitored over time to ensure its reliability as a relative reference for LUCID, by means of internal cross-checks between the nominal and alternative track-selection working points employed in Run 3. Figure 2a shows track selection efficiencies relative to a loose muon selection, evaluated in $Z \to \mu\mu$ events from 2023 pp data. The sample requires two isolated 'combined' muons with $p_{\text{T}} > 20$, GeV, reconstructed from matched tracks in the Inner Detector and Muon Spectrometer [7]. The resulting efficiencies are then applied as run-by-run corrections to TC measurements. In Figure 2b, the efficiency-correct ratios of integrated luminosity measurements obtained with alternative TC selections to the nominal one are shown. All selections are observed to be robust and stable in 2023, showing an internal agreement within 1%. Studies of TC stability in other Run 3 years are in progress.

3. Luminosity with Pixel Cluster Counting

A brand new Pixel Cluster Counting (PCC) algorithm is being developed in ATLAS for luminosity measurements in Run 3 of the LHC. A PCC algorithm is employed by CMS as its baseline luminometer [10], and earlier implementations were attempted in ATLAS using only a subset of modules in the innermost layer of the Pixel Detector [11, 12]. PCC measures μ_{vis} from the

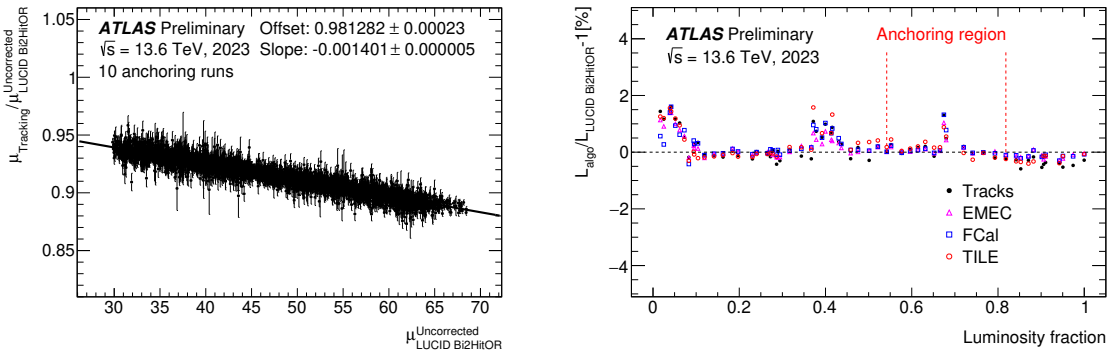

(a) **(b)**

Figure 1: (a) The ratio of $\langle\mu\rangle$ (equivalent to the ratio of instantaneous luminosity) measured by TC to that measured by LUCID, using the Bi2HitOR algorithm, as a function of the mean number of interactions per bunch crossing measured by the latter algorithm in 10 physics runs taken in 2023 in the vicinity of the vdM-scan period. The line shows the linear fit to the $\langle\mu\rangle$ ratio values [4]. (b) Fractional differences in run-integrated luminosity measurements with LUCID Bi2HitOR and other algorithms, including TC (black points), as a function of the fractional cumulative integrated luminosity in 2023. The anchoring region marks the range around the vdM-scan period from which ten runs are selected to derive the TC-based correction applied to LUCID in physics data-taking conditions [4].

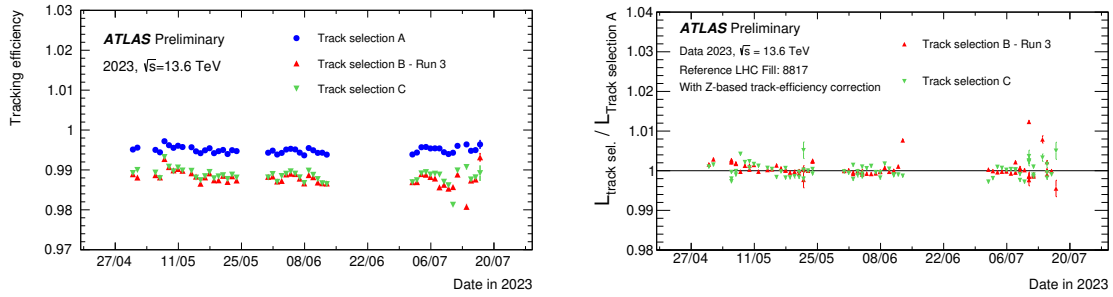

(a) **(b)**

Figure 2: (a) Track-selection efficiency for three different sets of selection criteria, during physics operation at high luminosity in 2023. The efficiency is measured using isolated muon candidates with $p_T > 25$ GeV in $Z \to \mu\mu$ events where the loose track selection from Ref. [9] is applied. Track selection A is built from the TightPrimary selection of Ref. [9] with additional requirements on $|d_0/\sigma_{d_0}| < 7$ and on the number of holes in the Pixel Detector, $N^{\text{Pix}}_{\text{holes}} \leq 1$. In track selection B - Run 3, the η range covers up to $|\eta| < 2.5$. Track selection C, based on selection A, has a uniform η request on the number of hits in the silicon detector, $N^{\text{Si}}_{\text{hits}} \geq 10$ [13]. (b) Time evolution of the run-integrated luminosity ratio determined with TC using selections A, B and C. The track selections are normalized in one reference run (LHC fill 8817, 23^{rd} August 2023) [13].

mean number of clusters per bunch crossing reconstructed in the ATLAS Pixel Detector, with pixel clusters defined as groups of adjacent pixels registering a signal above threshold in the sensors. The input data to the algorithm originate from the same readout stream and random triggers as TC, with an additional dedicated online selection to mitigate noise and background contamination. The current selection targets clusters reconstructed at high η in the Pixel barrel, which must satisfy

specific shape and charge requirements, ensuring good separation between luminosity-associated signal and background clusters: namely, cluster length > 1 pixel; total cluster size < cluster length + 5 pixels; cluster charge > 30 ke. Plots illustrating the cluster selection are provided in Figure 3.
The stability of PCC within a run (hours) was tested during periods of stable head-on collisions ($\langle\mu\rangle \sim 0.5$) in the 2022 ATLAS vdM fills, by studying the PCC/TC ratio of the visible interaction rate as a function of the TB number, after normalising PCC to TC at the start of the run. Following normalisation, an acceptance correction is derived in the same period to account for variations in the average longitudinal Beam Spot position over the considered TB numbers. The $\langle\mu_{\text{vis}}^{\text{PCC}}\rangle$ / $\langle\mu_{\text{vis}}^{\text{TC}}\rangle$ dependence on the Beam Spot location is characterised by fitting the ratio as a function of the average longitudinal Beam Spot position in each TB, as shown in Figure 4a. With the application of the longitudinal acceptance correction, good stability over time of PCC is observed. Figure 4b shows the evolution of $\langle\mu_{\text{vis}}^{\text{PCC}}\rangle$ / $\langle\mu_{\text{vis}}^{\text{TC}}\rangle$ over time for Layer-1 of the Pixel Detector.
A preliminary procedure to validate the time stability of individual Pixel modules has been developed using the normalised ratio of the number of pixel clusters in a single azimuthal module to the total number of clusters in the corresponding Pixel ring (PCC weight). Modules to be vetoed in the analysis are identified as those exhibiting large deviations from the average PCC weight over the duration of a run. Single-module stability studies based on PCC weight have been performed in LHC fills containing both low-μ and high-μ periods, as illustrated in Figure 5 for a stable module in Layer 1 of the Pixel Detector.
The major source of background in luminosity measurements with PCC is due to "afterglow" activity, consisting of out-of-time clusters induced by preceding collisions and originating from long-lived particle-cascade tails and material activation. Afterglow contamination is studied under tailored conditions, such as LHC ramp-up fills containing only a few isolated filled and colliding bunches, using special random triggers that also sample empty bunch crossings at an enhanced rate. Figure 6a shows the visible interaction rate measured by PCC with IBL 3D modules in 4 empty BCIDs before an isolated filled BCID and in 19 empty BCIDs after it. The initial 4 empty BCIDs do not contain afterglow by definition, as they occur before the filled bunch crossing (the localised enhancement visible in the figure is an IBL-related artefact). Instead, the activity in the second group of empty BCIDs contains the afterglow induced by the isolated filled bunch. This is well described by the sum of an exponential, accounting for the bulk of the afterglow activity, and a linear function, capturing an *intrinisc* background component and longer-lived residual activity, as shown in Figure 6b. This characterisation of afterglow represents a first step towards the implementation of a complete afterglow subtraction procedure for PCC in normal physics data-taking conditions.

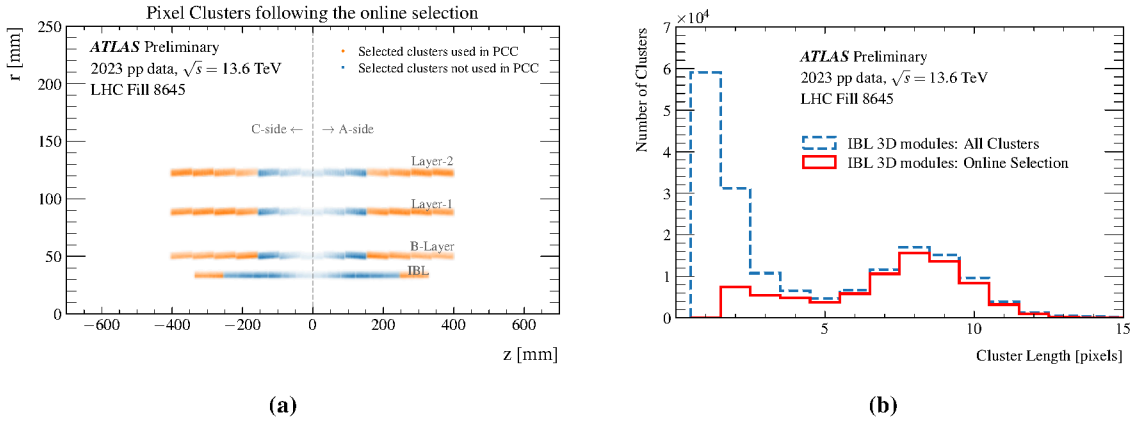

(a) **(b)**

Figure 3: (a) Distribution of the $(z,\ r)$ coordinates of the pixel clusters retained by the selection in use for the preliminary Run-3 PCC analysis (orange points), requiring clusters to be reconstructed in the central (barrel) region of the ATLAS Pixel Detector and having: length > 1 pixel; total cluster size < cluster length + 5 pixels; cluster charge > 30 ke. The orange points correspond to the coordinates of pixel clusters reconstructed in the longitudinal module-rings used in the analysis [13]. (b) Length of pixel clusters at high η in one of the Pixel-barrel layers, the IBL, before (blue histograms) and after (red histograms) the application of the cluster selection [13].

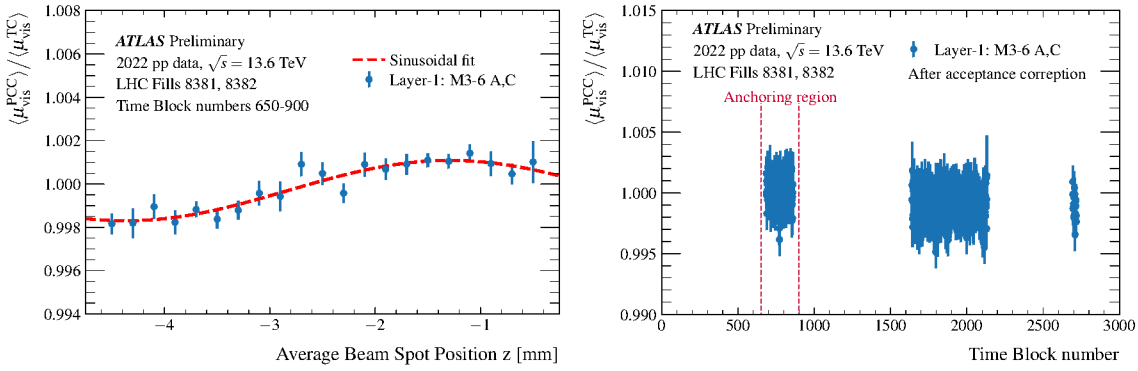

(a) **(b)**

Figure 4: (a) Ratios of the average visible interaction rates, $\langle\mu_{\text{vis}}\rangle$, measured by PCC with Layer-1 of the Pixel Detector and TC as a function of the average longitudinal Beam Spot position in the initial period of stable head-on collisions of the 2022 ATLAS vdM fills. Ratios are fitted with a sinusoidal function represented by the red dashed line in the plots [13]. (b) PCC/TC ratios of the average visible interaction rates as a function of TB number, in all periods of stable head-on collisions of the 2022 ATLAS vdM fills, after applying the longitudinal acceptance correction [13].

4. Summary

An accurate measurement of luminosity is a key component of the ATLAS physics programme, which aims at an ultra-precise final luminosity measurement in Run 3 of the LHC. Its success relies on the redundancy of stable and linear, independent luminometers, including those based on the Inner Detector, namely track counting (TC) and pixel cluster counting (PCC). TC is a well-established

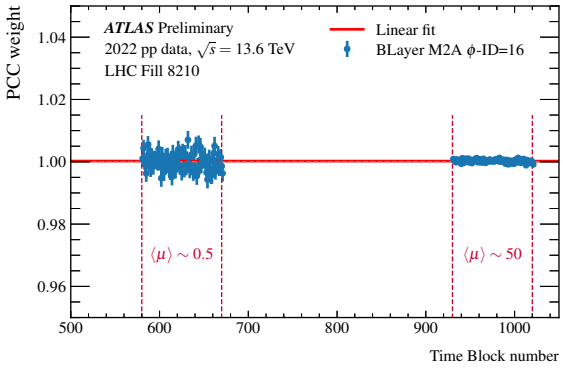

Figure 5: PCC weight for a module of the Pixel B-Layer as a function of TB number in a 2022 LHC Fill with head-on-collision periods at a low pileup ($\langle\mu\rangle \sim 0.5$) and high pileup ($\langle\mu\rangle \sim 50$), marked in the plot by dashed vertical red lines [13].

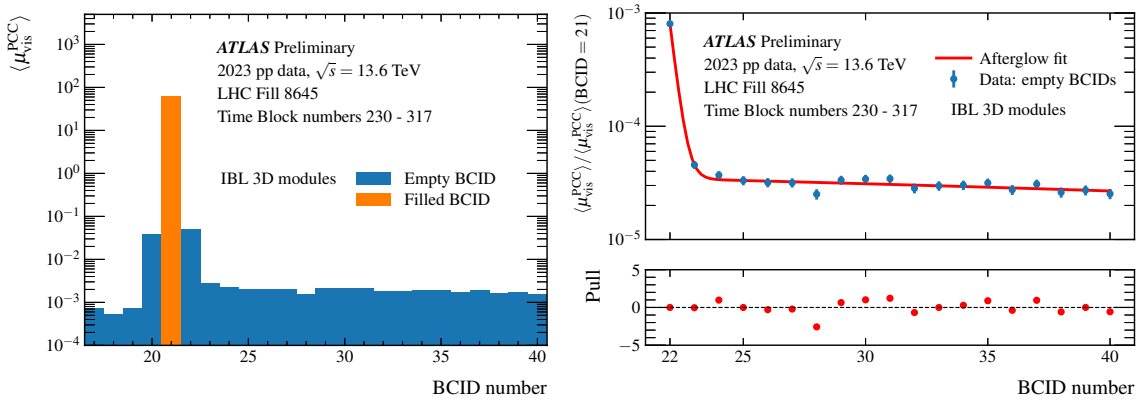

(a) **(b)**

Figure 6: (a) PCC visible interaction rate, $\langle\mu_{\text{vis}}^{\text{PCC}}\rangle$, measured using the IBL 3D modules, in the 2023 LHC Fill 8645, as a function of BCID number in a group of sampled BCIDs consisting of 4 empty BCIDs (bunch gaps, in blue) before the isolated filled BCID 21 (in orange) and 19 empty BCIDs after it. While the initial 4 empty BCIDs do not contain afterglow by definition, as they occur before the filled bunch crossing, the activity in the second group of empty BCIDs contains the afterglow induced by the isolated filled bunch [13]. (b) Fit to $\langle\mu_{\text{vis}}^{\text{PCC}}\rangle$ measured in the 19 empty BCIDs 22-40. In the figure, the values of $\langle\mu_{\text{vis}}^{\text{PCC}}\rangle$ are normalised to $\langle\mu_{\text{vis}}^{\text{PCC}}\rangle$(BCID = 21). The fit function consists of an exponential, capturing the pure afterglow contribution, plus a linear function describing an intrinisc background component and longer-lived residual activity. It is represented by the solid red line. The lower panel shows the pulls of the fit [13].

algorithm that provided crucial input to the Run-2 measurement [3], and continues to demonstrate good and stable performance also in Run 3. In parallel, the first implementation of a novel PCC algorithm in ATLAS is being developed in Run 3. Work is ongoing to provide the key inputs and tools for luminosity monitoring with PCC, and a preliminary analysis of Run-3 data already shows good performance of the new algorithm.

References

[1] ATLAS Collaboration, *The ATLAS Experiment at the CERN Large Hadron Collider*, *J. Instrum.* **3** (2008) S08003.

[2] L. Evans and P. Bryant, *LHC Machine*, *J. Instrum.* **3** (2008) S08001.

[3] ATLAS Collaboration, *Luminosity determination in pp collisions at $\sqrt{s}$ = 13 TeV using the ATLAS detector at the LHC*, *Eur. Phys. J. C* **83** (2023) 982.

[4] ATLAS Collaboration, *Preliminary analysis of the luminosity calibration for the ATLAS $\sqrt{s}$ = 13.6 TeV data recorded in 2023*, *ATL-DAPR-PUB-2024-001* (2024)

[5] S. van der Meer, *Calibration of the Effective Beam Height in the ISR*, *CERN-ISR-PO-68-31* **6** (1968).

[6] G. Avoni and others, *The new LUCID-2 detector for luminosity measurement and monitoring in ATLAS*, *J. Instrum.* **13** (2018) P07017.

[7] ATLAS Collaboration, *Muon reconstruction and identification efficiency in ATLAS using the full Run 2 pp collision data set at $\sqrt{s}$ = 13 TeV*, *Eur. Phys. J. C* **81** (2021) 578.

[8] ATLAS Collaboration, *The ATLAS experiment at the CERN Large Hadron Collider: a description of the detector configuration for Run 3*, *J. Instrum.* **19** (2024) P05063.

[9] ATLAS Collaboration, *Early Inner Detector Tracking Performance in the 2015 data at $\sqrt{s}$ = 13 TeV*, *ATL-PHYS-PUB-2015-051* 2015.

[10] CMS Collaboration, *Precision luminosity measurement in proton-proton collisions at $\sqrt{s}$ = 13 TeV in 2015 and 2016 at CMS*, *Eur. Phys. J. C* **81** (2021) 800.

[11] ATLAS Collaboration, *Pixel-Cluster Counting Luminosity Measurement In ATLAS*, *ATL-DAPR-PROC-2016-001* 2017.

[12] ATLAS Collaboration, *Proceeding Paper for HSTD11 Conference about Luminosity Measurement by Pixel-Cluster-Counting*, *ATL-DAPR-PROC-2018-001* 2018.

[13] ATLAS Collaboration, *Track Counting and Pixel Cluster Counting luminosity plots for the 2022-2024 pp $\sqrt{s}$ = 13.6 TeV running period*, *ATL-COM-DAPR-2025-016* 2025.

PoS(EPS-HEP2025)278